LASER PATTERNING OF CIGSE SOLAR CELLS USING NANO- AND PICOSECOND PULSES – POSSIBILITIES AND CHALLENGES

M. Schüle[1*], C. Schultz[1], V. Juzumas[2], K. Stelmaszczyk[1], M. Weizman[1], C. Wolf[2], N. Papathanasiou[2], B. Rau[2], R. Schlatmann[1,2], V. Quaschning[1], B. Stegemann[1], F. Fink[1]

[1] *PVcomB / HTW Berlin - University of Applied Sciences, Wilhelminenhofstr. 75a, 12459 Berlin, Germany*
[2] *PVcomB / Helmholtz-Zentrum Berlin für Materialien und Energie GmbH, Schwarzschildstr. 3, 12489 Berlin, Germany*
*Corresponding author: Manuel.Schuele@helmholtz-berlin.de, Phone: +49 30 8062 18156, Fax: +49 30 8062 15677

ABSTRACT: In this work we present results of different strategies of how CIGSe solar cells can be laser scribed focusing on P2 and P3. Therefore a laser source with a wavelength of 532 nm and pulse duration of 13 ns, as well as a laser, with pulse durations of 10 ps for both wavelengths of 532 nm and 1064 nm are used. The ablation mechanisms and the results ablation process (behaviors) due to different wavelengths and pulse durations are studied. Different parameters like process speed, scribe quality and solar cell performance are discussed. Successful laser patterning of all layers is demonstrated on a minimodule reaching 10% efficiency which is slightly better than the needle scribed reference.
Keywords: CIGS, Laser Processing, Ablation, Electrical properties

1 INTRODUCTION

Although laser patterning is well established in thin film solar cell manufacturing most times only the first (P1) patterning step in CIGSe solar cells is carried out by laser. The second (P2) and third (P3) patterning steps are still done mechanically by needle. Therefore one further step in driving down the production costs of CIGSe solar cells is to replace mechanical needle scribing by laser scribing. Advantages besides higher process control, less machine down time and therefore higher throughput is an increased solar module performance due to the possibility of reducing the dead area.

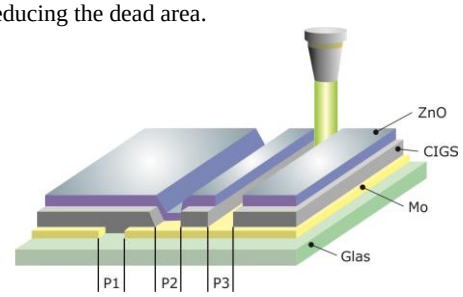

Figure 1: Schematic of monolithically inter-connected CIGSe thin film solar cell.

Figure 1 shows the three necessary patterning steps to achieve the monolithic series interconnection of single cells into a solar module. The first patterning step ablates the back contact and defines the cell width. The second patterning step removes the absorber so that an interconnection between back and front contact is created when the TCO layer is deposited. The third and last patterning step removes the TCO (and absorber) to isolate adjacent cells.

Nevertheless, laser patterning of CIGSe solar cells is still challenging. Ablation of molybdenum strongly depends on its layer properties and layer system [1]. For P2 and P3 laser patterning the risk of shunting the heat sensitive absorber is the most crucial factor. Therefore it is essential to apply appropriate laser ablation processes which depend on the individual layer structure. All laser patterning for a solar module has already been demonstrated [2].

In this work, laser with different wavelengths (532 and 1064 nm), different pulse widths (10 ps and 13 ns) and different ablation mechanisms are investigated in order to evaluate the possibilities and challenges of manufacturing high quality solar modules by laser scribing.

Table I: Patterning approaches under evaluation.

Laser wavelength, pulse width	P2	P3 TCO	P3 TCO + CIGSe
532 nm, 13 ns	✓	✓	-
532 nm, 10 ps	✓	✓	✓
1064 nm, 10 ps	✓	✓	✓

Table I gives an overview of the different patterning techniques under investigation. Note that ablation of TCO and absorber layer with 13 ns 532 nm and a high spot overlap is not under evaluation since the thermal impact creates large heat affected zones which drives down the solar cell performance.

2 EXPERIMENTAL

For laser structuring a high-speed motion system for high-precision laser processing (Rofin Baasel Lasertech) was used. This system consists of linear motor drives for x-y-stages which can be precisely moved at a speed of up to 1.2 m/s.

For laser structuring with nanosecond pulses the "SL 3 SHG PV" (Rofin Baasel Lasertech) was used operating at 532 nm and 2 W maximum. The laser is a Q-switched, diode-pumped solid state laser. The laser pulse duration is 13 ns and depends on the laser pulse repetition rate with a maximum of 400 kHz. For patterning with ps pulses a Time Bandwidth source was used, emitting 1064 nm as well as the frequency-doubled wavelength with maximum pulse durations of about 10 ps. The maximum power of 15 W is achieved for infrared radiation. The pulse repetition rate can be varied from

50 kHz to 8.2 MHz. Both laser beams possess Gaussian spatial intensity distributions.

The samples were prepared at PVcomB, the Competence Center for Thin-Film and Nanotechnology for Photovoltaics Berlin [3]. They were taken from its CIGS baseline based on the sequential process of sputtered precursor layers, evaporated selenium and a subsequent treatment in a rapid thermal annealing process. For comparison of the results to earlier experiments the samples were made with processes which were used in the baseline at the beginning of 2013. The samples are composed of 3.1 mm soda lime glass (SLG) substrate, 800 nm Molybdenum back contact, 2-3 µm CIGSe absorber layer, 40 nm CdS buffer layer and 1 µm ZnO:Al (including i-ZnO).

The laser patterned trenches were analyzed via optical microscopy (Carl Zeiss Axio Scope A1), profilometry (KLA Tencor D120) and I-V measurements (Super Solar Simulator from Wacom) which is a class AAA sun simulator equipped with four-point contacts.

3 RESULTS FOR P2 SCRIBING

3.1 P2 Scribing with 1064 nm, 10 ps

Patterning the absorber with a picosecond laser is expected to reduce thermal defects created by the laser pulses compared to longer pulse durations. Nevertheless ablation of the absorber (including CdS and i-ZnO) requires several laser shots on the same spot area for ablating the material down to the molybdenum. Since most of the laser energy is directly absorbed from the layer itself which is intended to be removed this process is called direct, multiple spot ablation.

In fact we achieved very promising results with a spot overlap of 99 % which corresponds to nearly 80 laser pulses per spot area. With a low fluence of 0.43 J/cm² we were able to produce a trench with a constant width of about 40 µm. Figure 2 and 3 indicate complete removal of the absorber layer, steep edges and a smooth bottom. The latter indicates that the molybdenum layer remains undamaged. It is also observable that there are some protruding heights on the sidewalls. Since they are quite low compared to the thickness of the TCO this does not have any negative influence.

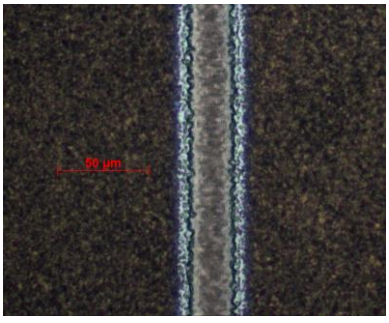

Figure 2: Microscopy image of laser patterned P2 trench with 10 ps and 1064 nm wavelength.

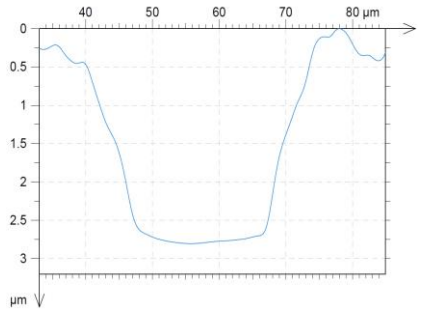

Figure 3: Profilometry scan of laser patterned P2 trench with 10 ps and 1064 nm wavelength.

Due to the high spot overlap of the laser pulses it is more appropriate to describe the process with respect to fluence and moving speed of the sample. This value called cumulated fluence was calculated to be 34 J/cm² for 1064 nm ablation. Moving speeds of more than 1000 mm/s were realized successfully.

Undamaged molybdenum is one indicator of a good P2 process. The results showed that it is advantageous to apply higher pulse energies in combination with a lower spot overlap for the same amount of cumulated fluence. Since the absorber is more transmissive at 1064 nm we conclude that a specific amount of the laser energy is absorbed at the back contact leading to a heat accumulation which gradually damages the molybdenum.

3.2 P2 Scribing with 532 nm, 10 ps

Just like 1064 nm the layers on top of the absorber are transmissive for green laser light. Therefore the same ablation mechanism is dominant as for 1064 nm. Figure 4 and 5 shows a micrograph and profilometry scan of a P2 scribe carried out with 10 ps and 532 nm wavelength indicating complete removal of the absorber layer.

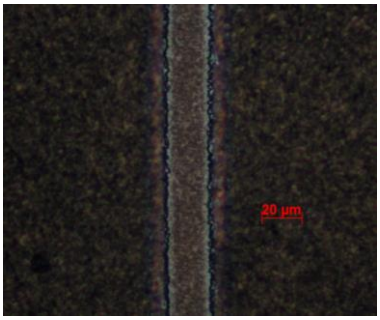

Figure 4: Microscopy image of laser patterned P2 trench with 10 ps and 532 nm wavelength.

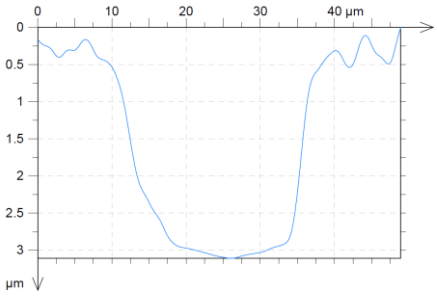

Figure 5: Profilometry scan of laser patterned P2 trench with 10 ps and 532 nm wavelength.

Similar to the P2 scribes done with 1064 nm wavelength the trench has a homogeneous appearance and a constant width of 40 µm. The ablation depth indicates that the CIGSe was removed completely and the clean bottom shows no indication of damaged molybdenum. The scribes were performed with a fluence of 0.16 J/cm² corresponding to a cumulated fluence of 43 J/cm².

Contrary to the scribes performed with 1064 nm wavelength we found that it is beneficial to apply lower pulse energies with a higher spot overlap for the same cumulated fluence. This is probably due to the lower optical penetration depth and necessary in order to avoid damage of the molybdenum back contact. Due to this, we reached maximum patterning speeds of only 150 mm/s.

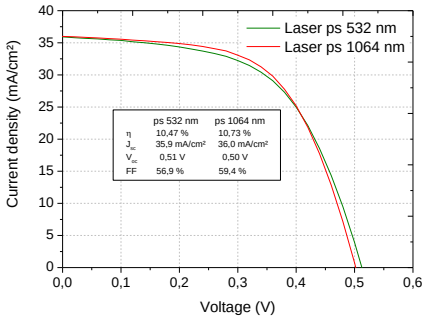

Figure 6: I-V curves of minicells P2 patterned with 10 ps, 532 nm and 1064 nm wavelength, respectively.

Figure 6 shows the I-V curves of two minicells. Their area is 0.6 cm² and the P3 was performed by needle for both of them. The P2 scribing was carried out with 532 nm for one minicell and 1064 nm wavelength for the other one. Both attempts show very promising results and yield a conversion efficiency of more than 10 %. The needle scribed references reached similar efficiencies.

3.3 P2 scribing with 532 nm, 13 ns

Another possibility of carrying out the P2 scribe is to utilize a laser source with pulse durations in the nanosecond time regime [4,5,6]. The approach with this setup is contrary to the ones with picosecond laser pulses since an ablation without tremendous melting zones is not possible for these pulse durations. Instead it is feasible to make use of the long pulse durations and to transform the absorber layer into a copper rich compound with high conductivity by creating binary phases. Since this process can be performed through the already deposited TCO layer it would help to further simplify the patterning process and to decrease the production costs.

In order to ensure high quality solar cells a fluence of 0.3 J/cm² and a spot overlap of more than 99 %, which corresponds to a cumulated fluence of around 33 J/cm² have shown very promising results. To avoid damages of the underlying molybdenum layer and to stimulate the creation of highly conductive phases we moved the laser spot out of its focus position in order to homogenize the Gaussian peak intensity. As already observed for patterning with 10 ps and 532 nm it is beneficial to apply lower pulse energies and higher spot overlaps.

Figure 7 shows the trench patterned through the window layer. The first laser shot results in ablation of the TCO layer. The width of this P2 scribe is less than 50 µm and therefore roughly 10 µm wider than the trenches scribed with the picosecond laser system.

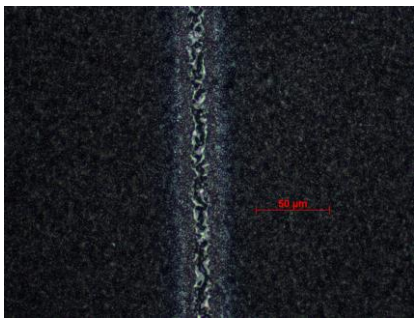

Figure 7: Microscopy image of phase transformed P2 trench carried out with 13 ns 532 nm.

Due to the high spot overlap of the laser pulses the process suffers from low scribing speed. Therefore we investigated how stable the process works with increased patterning speeds. Figure 8 shows a boxplot of the results. A box contains 50 % of the measured data points and the middle line inside the box is the median. The tips of the projecting bars show the minimum and the maximum values. The results clearly show that high efficiencies are achieved for patterning speeds up to 240 mm/s corresponding to an overlap of approx. 98 %.

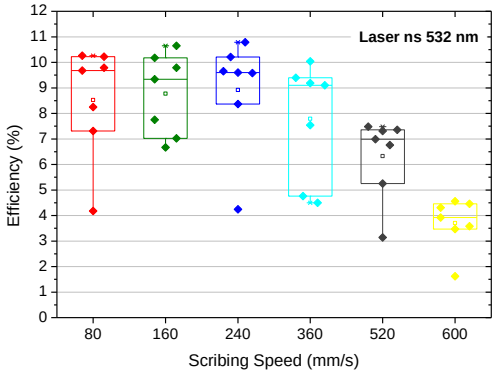

Figure 8: Efficiency boxplot of P2 patterned minicells with 13 ns 532 nm and different scribing speeds.

By moving towards higher speeds the cumulated fluence drops down and is not sufficient anymore for complete phase transformation. This finding is confirmed by the series resistances of the minicells which are plotted in Figure 9.

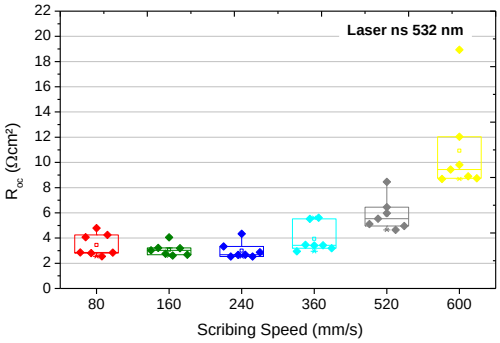

Figure 9: Series resistance boxplot of P2 patterned minicells with 13 ns 532 nm and different scribing speeds.

The results show that the lowest series resistance can be achieved for a scribing speed of approximately 200 mm/s. Lower values and therefore higher cumulated fluences applied to the layers result in damage of the back contact.

4 RESULTS FOR P3 PATTERNING

4.1 Selective TCO ablation

Removal of only the TCO layer is sufficient to achieve proper isolation because the absorber itself has a very low conductivity. The ablation mechanism for both 532 nm and 1064 nm wavelength is an indirect induced ablation [7]. TCO and CdS are nearly transparent for both wavelengths. Therefore the laser light is absorbed from the CIGSe layer leading to a material blast-off of all the layers above. This mechanism occurs for every single laser shot. Thus this process is called single spot ablation.

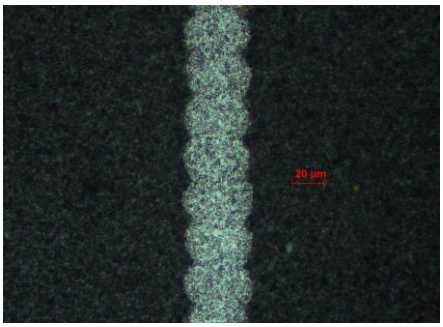

Figure 10: Microscopy images of 10 ps and 532 nm wavelength.

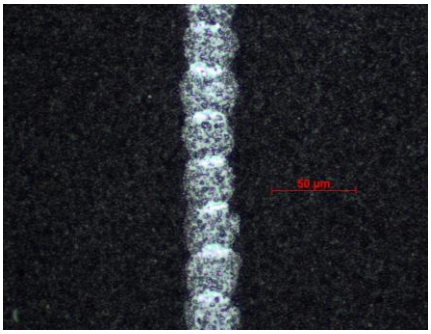

Figure 11: Microscopy images of 13 ns 532 nm ablation.

The differences between pico- and nanosecond laser ablation are shown in Figure 10 and 11. Ablation with shorter pulse duration results in more regular ablated areas than with longer pulse durations. In addition, clear melt formation in the overlapping areas of the spots can be seen for 13 ns 532 nm. We found that P3 scribes carried out with nanosecond laser lead to an overall solar cell performance drop by about 80%. Since this is also true for the open circuit voltage, we assume that the p-n-junction gets damaged severely.

For picosecond laser ablation instead, the quality of the scribe is significantly better und the width more constant. This is essential when for minimizing the dead area. Nevertheless, a drop of shunt resistance by about 50 % is observed for both wavelengths indicating that still binary phases are created which might reduce the solar cell performance.

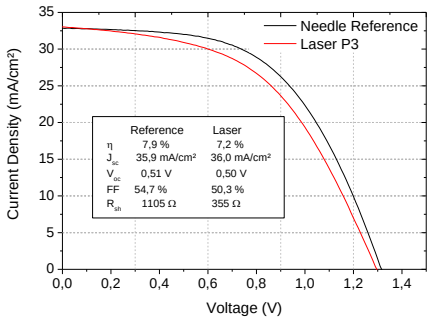

Figure 12: I-V curves of minimodules P3 patterned with needle (black) and laser 10 ps 532 nm (red).

Two minimodules, each of them consisting of three interconnected solar cells with a total area of 6 cm² were prepared. For both of them, P2 scribes were carried out with needle scribing. P3 however was performed with laser for one minimodule and the other was scribed with needle. The corresponding I-V curves are shown in Figure 12. The results indicate that the laser patterned P3 scribe still lacks of lower shunt resistance and a reduced efficiency of nearly 10 % compared to the needle scribed minimodule.

Concerning the scribing speed we were able to perform the P3 laser scribes with a maximum speed of 1.2 m/s. This value was only limited by the maximum speed of our stages within the patterning tool. The theoretical value which we estimated from upscaling the process by use of higher pulse repetition rates for 1064 nm is 7.5 m/s and for 532 nm it is 7.2 m/s.

4.2 Ablation of TCO and absorber

Another approach to carry out the P3 scribe is to remove TCO and absorber layer corresponding to the standard needle process. Especially in this process it is important to remove the layers without significant melting zones since aim of the P3 scribe is to isolate adjacent cells. Therefore we only focus on picosecond patterning for both wavelengths.

For ablation of all layers above the molybdenum a high spot overlap is necessary. A patterning speed up to 800 mm/s was realized successfully. Nevertheless, the process window of this patterning approach is rather small. There is only a small field where the absorber is fully removed creating a trench with nearly constant width and at the same time the molybdenum remains undamaged.

The electrical results were not satisfying because the laser patterned minicells suffer from low shunt resistances and also efficiencies of 30 % less than the references scribed by needle. This behavior was observed for both wavelengths. From SEM investigations we know that this is related to extended melting zones. They are created by the wings of the Gaussian energy distribution which shunts the solar cell and therefore reduces the solar cell performance.

5 ALL LASER PATTERNED MINIMODULE

To demonstrate that the obtained results are also true for minimodules of larger size we prepared samples consisting of 14 interconnected cells with a total area of 56 cm². For better comparison of the results both

minimodules have the same dead area of 300 µm. The results of an all laser patterned and a needle scribed minimodule for P2 and P3 are shown in Figure 13.

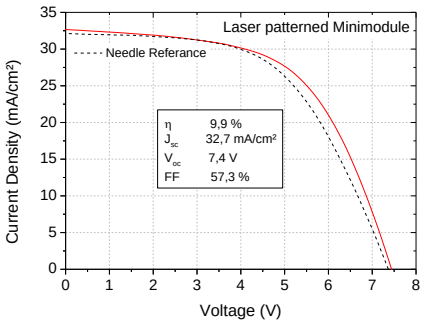

Figure 13: I-V curves of minimodules scribed with needle (black) and laser (red) with 13 ns 532 nm for P2 and 10 ps 532 nm for P3.

The laser scribed minimodule was patterned with the most promising technique from the experiments presented before. Accordingly, P2 was carried out with 13 ns 532 nm with a cumulated fluence of 33 J/cm² and P3 with 10 ps 532 nm and a fluence of 2.9 J/cm². The spot overlap for the laser P3 was calculated to be 4 % resulting in an overlap of the ablated spots of roughly 25 %. This result proves that the developed laser patterning processes are competitive to needle scribes.

6 CONCLUSION

We systematically investigated and evaluated several patterning approaches. We found that P2 patterning is feasible with all of the applied techniques: ablation of the absorber with picosecond pulses for both 532 and 1064 nm wavelength and phase transformation with nanosecond pulses for 532 nm. We demonstrated that successful removal of the absorber layer by multiple spot ablation is feasible with scribing speeds of more than 1000 mm/s. Concerning the third patterning step the results show clearly that the most promising approach is ablation of only the TCO. With this method scribing speeds of several meters per second are possible.

By further optimization of the laser processes, the laser setup and reduction of the dead area the fabrication of minimodules with efficiencies above 10 % is feasible.

ACKNOLEDGEMENTS

The Authors would like to thank all the people from PVcomB and HZB which were involved in cell preparation and measurements of the solar cells.

This work was supported by the Federal Ministry of Education and Research (BMBF) and the state government of Berlin (SENBWF) in the frame work of the program “Spitzenforschung und Innovation in den Neuen Ländern” (grant no. 03IS2151C).

REFERENCES

[1] C. Schultz, M. Schüle, K. Stelmaszczyk, J. Bonse, R. Witteck, M. Weizman, H. Rhein, B. Rau, R. Schlatmann, V. Quaschning, B. Stegemann, F. Fink, Proc. 27th EU-PVSEC, Frankfurt/M. (2012), 2266.

[2] B. Burn, C. Romano, M. Muralt, R. Witte, B. Frei, S. Bücheler, S. Nishiwaki, Proc. SPIE 8243, San Francisco (2012).

[3] B. Rau, F. Friedrich, N. Papathanasiou, C. Schultz, B. Stannowski, B. Szyszka, R. Schlatmann, Photovoltaics International 17 (2012), 99.

[4] P.-O. Westin, U. Zimmermann, M. Ruth, M. Edoff, Solar Energy Materials and Solar Cells, Vol. 95 (2011), 1062.

[5] C. Schultz, M. Schüle, M. Richter, H.-U. Pahl, H. Endert, J. Bonse, I. Dirnstorfer, B. Rau, R. Schlatmann, V. Quaschning, F. Fink, B. Stegemann, Proc. 26th EU-PVSEC, Hamburg (2011), 2943.

[6] B. Stegemann, M. Schüle, C. Schultz, H.-U. Pahl, J. Niederhofer, H. Endert, V. Quaschning, F. Fink, Laser Technik Journal, Volume 9 Issue 1 (2012), 25.

[7] G. Heise, M. Dickmann, M. Domke, A. Heiss, T. Kuznicki, J. Palm, I. Richter, H. Vogt, H. P. Huber, Applied Physics A 104 (2011), 387.